Mass divergences in annihilation processes. I. Origin and nature of divergences in cut vacuum polarization diagrams

George Sterman
Institute for Theoretical Physics, State University of New York at Stony Brook, Stony Brook, New York 11794
(Received 6 December 1977)

The origin of mass divergences in internal loop momentum integrals of cut vacuum polarization diagrams is investigated. It is found that loop momentum configurations which can give rise to mass divergences are of a severely limited form and have a direct interpretation in terms of physically realizable processes. A power-counting procedure suitable for estimating the nature of mass divergences is developed, and it is found that in a large class of field theories, cross sections smeared over a small region of phase space are at worst logarithmically divergent.

I. INTRODUCTION

Mass divergences in perturbation theory have been a topic of continuing interest. This is due in large part to their importance in field theories with unbroken gauge symmetries, such as quantum electrodynamics and quantum chromodynamics.[1] In addition, at sufficiently high energies, the concept of mass divergences becomes relevant even to theories with only massive particles.[2] The classic work of Kinoshita[3] and Lee and Nauenberg[4] made it clear that for many purposes it is possible to approach the question of mass divergences in a theory-independent way. In particular, the cancellation of mass divergences in appropriately defined cross sections already familiar from QED (Ref. 5) was seen to be a universal feature of field theories.

It is the purpose of this work to study mass divergences in single-photon annihilation processes directly in terms of the momentum-space behavior of Feynman integrals. The study is divided into two parts. In the second,[6] ensembles of annihilation final states are identified, whose cross sections are free of mass divergences. The first part deals with the origin of mass divergences in phase-space integrals and the internal momentum integrals of vertex functions. It is found that they can arise from only a very restrictive class of loop momentum configurations, which have a simple physical interpretation. A power-counting procedure is then developed for such momentum configurations. Assuming the validity of this procedure, we find that all mass divergences are logarithmic when cross sections are smeared over a small portion of phase space, as is inevitable experimentally. Much of the reasoning is theory independent. The power-counting result, of course, depends on the theory, but it extends to theories with four-scalar, Yukawa, and gauge couplings. It can be extended to include $(\phi^3)_6$ and gravitational theories as well, but this will not be done here.

This approach contrasts with studies based on parametric representations of Feynman integrals,[3,7] but is related to the usual treatment of infrared divergences in QED.[5] The momentum-space approach is attractive in its simplicity and for the rather direct physical interpretations which it suggests. It has the disadvantage that it does not incorporate directly the global properties of Feynman integrals. For instance, those having to do with ultraviolet divergences will be largely ignored in the following; I simply assume that approriate counterterms can be found to make the theory finite. All renormalization is assumed to have been done "off-shell" in such a way as to introduce no new mass divergences.

The cross sections for single-photon annihilation processes are given by cut vacuum polarization diagrams via unitarity. From graph G, a state α gets the differential contribution

$$d\sigma_\alpha^{(G)} = \Gamma_L^{(\alpha)} d\tau^{(\alpha)} \Gamma_R^{(\alpha)*}, \tag{1.1}$$

where $\Gamma_L^{(\alpha)}$ and $\Gamma_R^{(\alpha)}$ are the vertex functions generated by cut α of G, as in Fig. 1. $d\tau^{(\alpha)}$ represents the phase-space measure of α, including possible spin factors. As mentioned above, any experimental procedure does not measure quantities such as (1.1) directly, but at best those such as

$$\Delta\sigma_\alpha^{(G)} = \int_{\Delta_\alpha} \Gamma_L^{(\alpha)} d\tau^{(\alpha)} \Gamma_R^{(\alpha)*}, \tag{1.2}$$

where Δ_α is some small region in α phase space. Quantities such as (1.2) will be referred to as partially integrated exclusive cross sections, and will be shown to be at worst logarithmically divergent.

Section II will deal with generalities on mass divergences, considered from the point of view of integration over Feynman diagram loop momenta. In Sec. III these results are applied to vertex func-

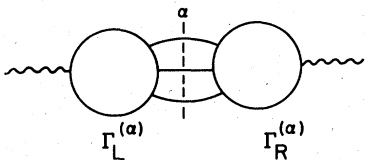

FIG. 1. General process to be considered.

tions which describe the decay of a timelike photon. In Sec. IV a power-counting procedure is developed which is appropriate to regions in momentum space from which mass divergences arise, and in Sec. V power counting is used to show that partially integrated exclusive cross sections are at worst logarithmically divergent. An appendix deals with power counting in more general situations. Except where otherwise noted, the discussion is for totally massless theories.

II. THE MOMENTUM-SPACE STRUCTURE OF MASS SINGULARITIES

The amplitudes $\Gamma_{L(R)}^{(\alpha)}$ in (1.1) are represented by graphs, which can be split into maximal one-particle irreducible (1PI) subgraphs and tree subdiagrams. The external momenta of each graph are, of course, real and physical. Mass singularities must arise from the vanishing of denominators at special values of phase space and loop momenta. I will first discuss how this happens in 1PI subdiagrams. The discussion centers on analyticity properties of Feynman integrals and as such is theory independent.[8]

Mass singularities in 1PI subdiagrams

Each Feynman integral is originally given as a multiple integral over real loop momenta, but the $i\epsilon$ conventions which help define these integrals make it necessary to consider them as contour integrals in a multidimensional complex space. The original real values of the loop momenta are said to lie on the "undeformed" contour in this space.

Along the undeformed contour, the integral will in general encounter points where Feynman denominators vanish, and at which the integrand consequently diverges. Call any such point a "singular point" (SP). While there must be singular points for there to be mass singularities or

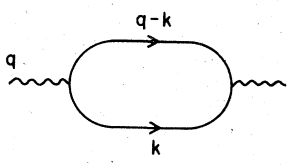

FIG. 2. Simple example discussed in text.

divergences, not every SP is directly associated with these phenomena. As a trivial example, consider the vacuum polarization graph Fig. 2. Whether or not the lines k and $q-k$ have a nonvanishing mass m, when $q^2 \neq 4m^2$, the corresponding Feynman integral is well defined. This is so despite the fact that SP's at which $k^2 = (q-k)^2 = m^2$ are easily found along the undeformed k contour. The reason for this is that the k contour is not *pinched* at any such SP. (Because the k contour is infinite, it can be trapped at a point only where it is pinched there between a pair of coalescing singularities.) As a result, the k contour integral can be evaluated without ever encountering such SP's at all.

It is only singular points at which the undeformed contour is pinched that can give rise to mass divergences—as well as more general singularities which may be associated with massive particles. To distinguish them, these points will be called "pinch" SP's. The search for mass divergences in any given process can begin with a catalog of pinch SP's in graphs relevant to that process. At this point it is useful to develop certain general observations about pinch SP's, not dependent on the masses of particles involved.

With each SP, pinch or not, is associated a reduced diagram, constructed from the complete graph by simply contracting all lines which are off-shell at the SP. The reduced diagrams of pinch SP's will be seen below to have particularly simple structure in certain cases of interest. Quite generally, in fact, the reduced diagrams of pinch SP's have a direct physical interpretation when external momenta are physical. This was observed by Coleman and Norton.[9] Part of their analysis, modified slightly to incorporate massless particles, is outlined below.

Physical picture for pinch singular points

Let P be an SP with reduced diagram R. At P each line in R has a definite on-shell momentum. The lines and loops of R are classified into subsets as follows. Let F and G be the set of finite-momentum and zero-momentum lines of R, respectively. (Lines in G are of necessity massless.) The loops of R are also assigned to fall into two classes. Those in set A pass through lines in F only, and they are chosen to form an independent set of loops of the subgraph of R formed by lines in F. The remaining loop momenta, set B, all vanish. Lines in G carry only loop momenta from B.

Feynman parameters can be used to illustrate how the momentum contour is trapped at P. Parametrizing only denominators in F gives, for the Feynman integral, a quantity with the structure

$$\int \prod_{k\in B} d^4k \prod_{i\in G} [q_i^2(k)+i\epsilon]^{-1} \int_0^1 \prod_{i=1}^{n_F} d\alpha_i \delta\left(\sum_{i=1}^{n_F} \alpha_i - 1\right) \int \prod_{l\in A} d^4l \left[\sum_{i\in F} \alpha_i (q_i^2(k,l) - m_i^2) + i\epsilon\right]^{-n_F}, \tag{2.1}$$

where n_F is the order of F, and any set of masses m_i may vanish. Numerator momenta, which do not enter into the argument, have been suppressed.

Look at the l and α integrations for fixed k near 0. Diagonalizing the last denominator in terms of the l loop momenta gives

$$\int \prod_{k\in B} d^4k \prod_{i\in G} [q_i^2(k)+i\epsilon]^{-1} \int \prod_{i=1}^{n_F} d\alpha_i \delta\left(\sum_{i=1}^{n_F} \alpha_i - 1\right) \int \frac{d^{4L}l'}{C_F^2(\alpha)} \left[l'^2 + \frac{D_F(\alpha,p,k)}{C_F(\alpha)} + i\epsilon\right]^{-n_F}, \tag{2.2}$$

where $C_F(\alpha)$ and $D_F(\alpha,p,k)$ are standard functions defined, for instance, in Ref. 10, and constructed for for the subgraph of R consisting of lines in F. p represents the external momenta and L is the number of loops in A. The SP P is at $k = l' = D_F = 0$ in (2.2).

First of all, the $k\in B$ are trapped at $k = 0$ independently of the l' and α integrations: Every denominator $q_i^2 + i\epsilon$ supplies a double pole pinching each contour at the origin. Next, the l' integral can be evaluated explicitly to give an inverse power of D_F. It is worth noting, however, that the l' integral diverges at $D_F = 0$ because the l' contours are trapped at the origin as D_F vanishes. Finally, the α integrals themselves will be pinched at values for which $D_F = 0$, if the Landau equations[10]

$$\begin{aligned} &q_j^2 = m_j^2, \quad j\in F, \\ &\sum \alpha_i q_i = 0 \end{aligned} \tag{2.3}$$

are satisfied with positive α's and real q's, with the sum taken around each loop of finite-energy lines.

It was necessary to separate the zero-momentum lines in order to obtain (2.3) for finite-momentum lines, just because any loop k, say, which appears in a denominator $k^2 + i\epsilon$ is always trapped at $k = 0$, regardless of other loops and lines. This is reflected in the fact that the analog of the Landau conditions (2.3) can be trivially satisfied for any loop, one of whose lines is massless and has zero momentum.

Coleman and Norton[9] pointed out that the momenta at the pinch SP P describe a physical process in which each vertex of R can be associated with a space-time point, separated by intervals proportional to the vectors $\alpha_i q_i$. The constant of proportionality may be fixed for the entire diagram at once, or separately for subdiagrams which share only loops in B with each other.

For massive lines, α_i is interpreted as the ratio of the proper time separating the line's emission and absorption to its mass. For massless lines such an interpretation is no longer possible, but α_i can still be viewed as the frame independent ratio of time elapsed to energy. Zero-energy lines have no restrictions from the Landau equations, and this makes sense in terms of the infinite wavelength corresponding to such lines. Vertices which connect only zero-momentum lines have arbitrary positions in this space-time picture.

Vertices of reduced diagrams

Because the reduced diagrams of pinch SP's describe physically realizable processes, it makes sense to classify vertices into two sets, which characterize the nature of the "event" which each vertex represents. (1) "Soft" vertices connect zero-momentum lines and/or a set of finite-energy lines at threshold in both incoming and outgoing states. The finite-energy lines connected at a soft vertex must be all massless or all massive. If the finite-energy lines at a soft vertex are massless, they have collinear spatial momenta, and if massive they are relatively at rest. The action of a soft vertex therefore preserves the flow of spatial momentum. Any number of zero-momentum lines can attach to a soft vertex. (2) Any vertex connecting lines whose momenta are above threshold in either the incoming or outgoing state is called "hard."

In terms of the physical picture developed above, soft vertices possess what might be described as "translation invariance." The replacement

$$\alpha_i q_i \to \alpha_i' q_i = \alpha_i q_i + \Delta q, \quad \alpha_i' > 0 \tag{2.4a}$$

for every incoming line at any soft vertex along with

$$\alpha_j q_j \to \alpha_j' q_j = \alpha_j q_j - \Delta q, \quad \alpha_j' > 0 \tag{2.4b}$$

for each outgoing line leaves the Landau conditions (2.3) satisfied. [Δq, of course, must be proportional to every q_i and q_j, which therefore must themselves be proportional and the vertex soft if (2.4a) and (2.4b) are to be satisfied.] Such a variation shows that the position of a soft vertex V is not fixed, but may vary anywhere along the interval connecting the last emission of a line absorbed at V and the first absorption of a line

emitted at V.

Tree subdiagrams

On-shell tree subdiagrams fall into the same physical picture. The vertices of any tree diagram can always be ordered so that the diagram realizes a physical process when external momenta are real and physical. As with zero-momentum lines, the lack of constraints analogous to (2.3) corresponds to the fact that the scale of separation between each pair of connected vertices is arbitrary.

III. PINCH SINGULAR POINTS OF CUT VACUUM POLARIZATION DIAGRAMS

In this section I will discuss simple consequences of the results of Sec. II for cross sections calculated from cut two-point functions via unitarity. The idea is to look for pinch SP's in vertex functions (all describing $1\to n$ processes) which are generated by cutting an arbitrary timelike two-point graph. The form of such pinch SP's will be seen to be strongly restricted by the foregoing considerations. Here, as in the preceding section, the results do not depend on the details of the theory used to generate the graphs in question (aside, of course, from the masses involved).

Massless theory

Suppose G is a graph in a massless theory, with a single incoming line of timelike momentum q and a number of on-shell outgoing lines. I will refer to G as a "decay" graph. The results of Sec. II lead easily to the following.

Lemma. Let P be a pinch SP of massless decay graph G with reduced diagram R. Suppose the external momentum q enters G at vertex V_q. Associate with R and P a physical process as in Sec. II. Then, among vertices of R through which finite energy flows, V_q is the one with earliest time, and every other vertex in R is soft.

Proof. V_q is first because in a physical process energy flows forward in time, and V_q is the only source of positive energy in R.

Consider the finite-energy internal lines of R which emerge from V_q. If two such lines l_1 and l_2 reinteract, they will do so at some vertex V'. Both V_q and V' are associated with points in space-time, say x_q and x' $[x_q^0<(x')^0]$. Since l_1 and l_2 begin and end at the same space-time point, their spatial momenta must be collinear. The particles associated with l_1 and l_2 are to be pictured as both being emitted at V_q, traveling with the speed of light in the direction of $\vec{x}-\vec{x}_q$, and finally being reabsorbed after a time $x_q^0-(x')^0$ has elapsed. Thus, finite-energy lines emerging from V_q can only reinteract if they have collinear spatial momenta, and their interactions take place only at soft vertices. But soft vertices preserve momentum flow, so finite-energy lines emerging from soft vertices can still only reinteract with the same set of collinear lines, coming either from V_q or subsequent soft vertices. Zero-momentum lines can be emitted or absorbed anywhere in R, but all resulting vertices are by definition soft.

This lemma results in a particularly simple physical picture, which must be satisfied by the reduced diagram of a pinch SP in any massless decay graph, and which can be summarized in the following points.

(a) The spatial momentum flow is determined at the initial vertex V_q. After V_q, only such interactions occur which leave not only the total momentum conserved, but also the quantities $\sum_i|k_i^\mu|$ where the sum is over all lines which coexist at any particular time after the action of V_q.

(b) Aside from V_q, possible vertices are all soft, describing the scattering of collinear finite-momentum lines or the emission, absorption, and scattering of zero-momentum lines.

(c) The reduced diagram may then be considered to describe the evolution of a series of states. Each such state will consist of a set of "jets" of finite-momentum lines as well as a "cloud" of zero-momentum lines. The number and individual energies and momenta of the jets are conserved by the action of soft vertices, and thus are the same in each state, including the final state, although the number of finite-momentum lines which make up any jet will depend on the state in general. Figure 3 illustrates a typical physical process satisfying points (a)–(c).

(c) implies that the momenta of the cut lines of a vacuum polarization diagram determine the number, energies, and directions of jets to be the same at the pinch SP's of both the right-hand and left-hand vertex functions in an expression such as (1.1). This enables one to speak of pinch SP's of the cut vacuum polarization graph, speci-

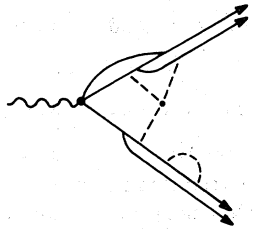

FIG. 3. Illustration of a reduced diagram with two jets, represented by sets of nearly parallel unbroken lines. Soft lines are represented by dashed lines. All vertices may involve contracted off-shell lines.

fied by a point in the cut phase space as well as by a pinch SP for each vertex function. It should be noted, however, that such a point is *not* a pinch SP for the uncut graph. In any case, these are the pinch SP's of the integrals of phase-space averaged exclusive cross sections.

Space-time picture of mass divergences

Referring to Fig. 3 we see how the set of jets realized at a pinch SP with reduced diagram R is associated with a set of subgraphs $\{r_j\}$ of R whose elements are connected only at V_q. Assigning loop momenta according to the scheme described in Sec. II, the r_j share only zero-momentum loops, and the space-time scale associated with each jet in the physical picture may be chosen separately. In addition, in Sec. II the "translation invariance" of all soft vertices was noted. This means that if v_i, v_{i+1}, v_{i+2} are consecutive vertices in a given jet subdiagram or in the subdiagrams of zero-momentum lines of R, then *any* physical picture where v_{i+1} occurs between v_i and v_{i+2} is equally acceptable.

These observations lead us to a space-time picture in which mass singularities manifest themselves as scaling freedom in the physical processes associated with pinch SP's. In Fig. 3, V_q represents off-shell processes which take place within a limited space-time region, and which determine the distribution of momentum in the physical state which will eventually develop. Once this disribution is realized, interaction does not cease, but involves no new finite-momentum transfers. It occurs only between collinear finite-momentum lines moving away from V_q with the velocity of light, and via zero-momentum (infinite wavelength) lines. The space-time positions of the vertices which describe these interactions can be scaled to infinity independently for each jet, and also independently within each jet (if the direction in time of lines is preserved). The space-time position of vertices connecting zero-momentum lines is completely underdetermined, and may lie at any point before or after V_q. These two kinds of scaling freedom correspond to "collinear" and "infrared" divergences, respectively.

Inclusion of massive particles

The introduction of massive lines[11] into the theory complicates the situation considerably because associated finite-energy thresholds lead to a much less restrictive structure for physical processes corresponding to pinch SP's. It is easy, however, to identify general properties of pinch SP's in certain interesting situations, particularly

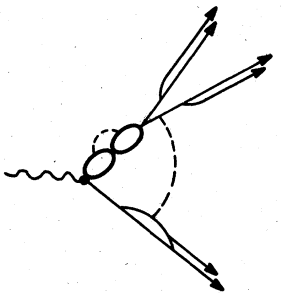

FIG. 4. Reduced diagram with internal massive lines at threshold and three external jets.

the massive pair production form factor at low-energy.

For simplicity, assume a single species of massive particle which, because it carries some conserved quantum number, must be created in pairs. Pinch SP's will be identified by examining possible physical processes, as above, for various ranges of the initial invariant q^2.

$0<q^2<4m^2$. In this range, massive particles appear neither in the final state nor, because of energy conservation, in any foregoing state in the reduced diagram of a pinch SP. So, below threshold, massive lines are never pinched on-shell in the Feynman integral, and the reduced diagrams of pinch SP's here are just the same as in the massless case.

$4m^2 \leq q^2 < 16m^2$. Suppose first that the final state is all massless. Let P be a pinch SP of diagram R, and go back to the reasoning of the lemma, considering the first physical state S of R after the vertex V_q. If all the lines in S are massless, no massive lines can ever be produced in a later state, since this would require non-collinear lines to interact (at a hard vertex), an event which cannot occur in a physically realizable process when these lines all emanate from the same space-time point (V_q). Therefore, if massive lines are to show up in R at all, they must be present already in S.

By assumption, the pair annihilates at some later vertex V'. To travel together between the two space-time points corresponding to V_q and V' the two lines must be relatively at rest—that is, at the two-particle threshold—in S and in all succeeding states. Of course, between V_q and V' they may interact any number of times with zero-momentum lines and with each other at four-point vertices. Their annihilation at V' is easily seen to give rise to a new set of jets of finite-energy massless lines which cannot "catch up" with any of the lines of jets emitted at V_q. For an example, see Fig. 4. In summary, massive lines may occur only in the form of a "bound

state" propagating from V_q to a later vertex V' where it "decays" into a new set of jets of massless lines. V_q and V' are the only hard vertices in R.

Now consider the situation when the pair of massive lines appears in the final state above threshold. Here the only hard vertex is V_q and each massive line acts individually as a jet, interacting only with massless lines. There may, of course, be jets of massless lines in R as well, also emanating from V_q, if they appear in the final state.

Of special interest are the pinch SP's of the massive pair form factor, where no massless lines appear in the final state. Because V_q is the only hard vertex, there are no finite-momentum massless lines at all in R. In terms of the physical picture, this is because any jet of finite-momentum lines emitted from V_q would simply "outrun" the massive lines and appear in the final state. The massive lines are also moving apart so that they cannot reinteract at a point to emit or absorb finite-energy massless lines. In R all massless lines have zero momentum, and "collinear" divergences play no direct role, even in the presence of mutual interaction of the massless lines. This case has been discussed elsewhere from this point of view.[12]

$16m^2 \leq q^2$. Above the four-particle threshold the situation is complicated by the possibility of multiple "bound states." It is easy to see that many hard vertices can arise as the "decay" products of these bound states interact, so that very complicated physical processes may be generated. All such processes must begin, however, with sets of massive lines at threshold in S.

Example

A simple illustration of the foregoing ideas is supplied by the triangle diagram with all massless lines. Its reduced diagrams with two or more lines are shown in Fig. 5 where heavy and dashed lines represent off-shell and zero-momentum particles, respectively. Of these four cases, (a)–(c) correspond to pinch SP's, while (d) does not.

Dropping any numerator factors, the Feynman integral is of the form

$$\int \frac{dk_0 dk_3 d^2\vec{k}}{(k_0^2 - k_3^2 - \vec{k}^2 + i\epsilon)[(k_0+Q)^2 - (k_3+Q)^2 - \vec{k}^2 + i\epsilon][(k_0-Q)^2 - (k_3+Q)^2 - \vec{k}^2 + i\epsilon]}, \tag{3.1}$$

where we have chosen a frame where $p_0 = p_0' = p_3 = -p_3' = Q$ and $|\vec{p}| = |\vec{p}'| = 0$. Except where otherwise noted, vector notation will be reserved for two-dimensional "transverse" vectors.

At the pinch SP's, where k is either zero or proportional to p or p', $\vec{k} = 0$ in the chosen frame. Consider, for example, the pole structure of the k_1 plane. Each denominator in (3.1) is of the form $d_i - k_1^2 + i\epsilon$, and the k_1 poles are at $\pm(d_1^{1/2} + i\epsilon)$. That is, poles at positive (negative) values of k_1 are always in the upper (lower) half-plane. The same, of course, is the case for k_2. We can choose the k_1 contour as in Fig. 6, where it crosses the real axis only at the origin. With this choice of contour, the SP's corresponding to Fig. 5(d) never occur at all. On the other hand, at each of the pinch SP's the k_1 contour is pinched at the origin. Thus, by deforming the contour, an integral is found whose only SP's are the pinch SP's.

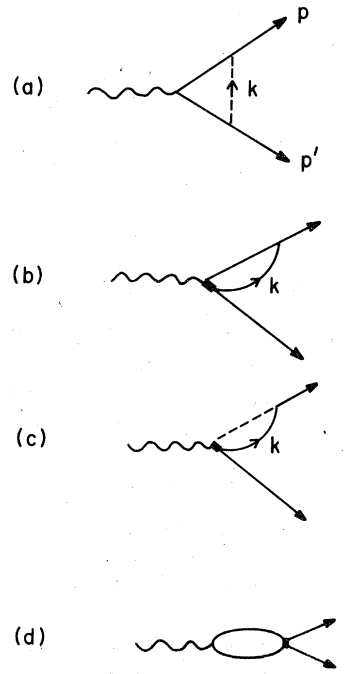

FIG. 5. Reduced graphs for SP's of the triangle diagram.

IV. BEHAVIOR OF INTEGRALS NEAR PINCH SP's: POWER COUNTING

So far I have identified the pinch SP's which occur in vertex functions generated by cutting vac-

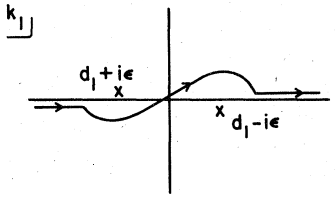

FIG. 6. Contour in k_1 plane which avoids SP's of reduced diagram Fig. 5(d).

uum polarization diagrams. In the following I look at the effect of pinch SP's on phase-space averaged exclusive cross sections, and show that mass divergences in these cross sections are at worst logarithmic in a massless theory. In addition, I will derive limitations on the structure of those pinch SP's, as illustrated by their reduced diagrams, which can give rise to logarithmic mass divergences.

To arrive at these results it will be necessary to apply power counting to the behavior of momentum integrals, both phase-space and internal loop, near pinch SP's. An obvious difficulty with this approach is that, for Feynman denominators in Minkowski space, $k^2=0$ does not imply $k=0$, so that naive dimensional counting will not necessarily bound the true behavior of the integral. As a result, it will be necessary to find a more appropriate power-counting scheme based on variables more closely related to the structure of the integral.

The choice of these "natural" variables is made possible by the observation that, if the freedom to deform loop momentum contours except at pinch SP's is used, cancellations in Feynman denominators will occur *only* at pinch SP's. A catalog of pinch SP's relevant to cut vacuum polarization graphs was made in the preceding section and is illustrated by Fig. 3 for massless theories. The structure of their reduced diagrams, consisting of jets and soft lines with hard vertices only where the external momenta attach, will suggest the appropriate choice.

The aim is to change variables and approximate the integral near the pinch SP in questions so that every denominator is a homogeneous function of a set of variables which vanish there. This will be referred to as the "homogeneous integral." Such variables will be called "normal" variables, and will be distinguished from the remaining variables, which will be referred to as "intrinsic." The terminology comes from the fact that pinch SP's are not isolated; rather, they lie on surfaces in momentum space. At any pinch SP, the intrinsic and normal variables parametrize the surface and its normal space, respectively. For instance, k_1 and k_2 were normal variables for the pinch singularity surfaces in the triangle diagram, while $k^+=k_0+k_3$ was an intrinsic variable for the surface corresponding to the reduced diagram of Fig. 5(b), when k is proportional to p. Similarly, for an integral in Euclidean space, the only SP's (which are all pinch SP's) are those at which the momenta of some set of lines vanish in all four components, and here the normal variables can be chosen as all components of the loop momenta of the reduced diagram, and the intrinsic variables as all other loop momenta. Power counting will directly involve only normal variables. The homogeneous integral will still encounter various singular points where internal cancellations occur among the variables in subsets of the denominators. But again, if contours are deformed when necessary, such cancellations will occur only when the integral is pinched at the corresponding SP. If power counting is carried out for an arbitrary SP, the behavior of the integral near this SP will already be bounded. This last point is implicit in dimensional counting for Euclidean integrals as well. In fact, from this viewpoint, the Wick rotation that makes dimensional counting possible for vertex functions with Euclidean external momenta is a special case of the deformation of contours referred to above.

Let $x_1,\ldots,x_m$ and $y_1,\ldots,y_n$ denote the intrinsic and normal variables, respectively, near pinch SP P. The homogeneous integral J near P will be of the form

$$J\sim\int_C\prod_{i=1}^{n}dy_i y_i^{-a_i}\int\prod_{j=1}^{m}dx_j I(\{x\},Y)\,, \tag{4.1}$$

where the hypercontour C passes through the point $y_1=y_2=\cdots=y_n=0$. Y represents the set of ratios formed from the y's. The power-counting estimate of the integral's behavior at P is found by scaling the normal variables y with a scale λ:

$$J\sim\int d\lambda\lambda^{p-1}\,,\quad p=n-\sum_{i=1}^{n}a_i\,. \tag{4.2}$$

We will see that for partially integrated exclusive cross sections, $p\geq 0$ and divergences are at worst logarithmic.

It should be pointed out that there may be pinch SP's in the homogeneous integral which are not pinch SP's of the true integral before nonleading terms have been dropped. This can happen when, in the complete integral, two poles do not quite pinch the contour, but are separated only by second-order terms. Such a situation corresponds to enhancements of the integral, as will be seen below. The extent of these "spurious" SP's in the homogeneous integral is a measure of the success with which the variables parametrize the normal space of the singularity surface. The variables

given below are chosen to minimize the spurious SP's.

Information about the particular field theory in question was not used in Sec. II. In the process of estimating integrals, however, properties of the theory such as the order of the vertices and spin of its particles will play an important role. Also, it will sometimes be necessary to examine the integral after certain loop momenta have been integrated over. For instance, sometimes it is useful to integrate the internal momenta of two- or three-point subgraphs in a reduced diagram. Notice that the only pinch singular points which will be encountered in these internal integrals are ones for which subsets of the internal lines of the subgraph are collinear to its external lines.

For power-counting purposes, the δ functions which set cut lines on-shell will be treated in the same way as Feynman denominators. Normal variables will be chosen for an arbitrary pinch SP of the cut vacuum polarization graphs (not for vertex functions individually), since these are the pinch SP's of the integrals from which are derived the phase-space averaged exclusive cross sections. Mass-shell δ functions act to eliminate a number of normal variables equal to the number of cut lines (leaving over a factor proportional to the inverse product of the cut lines' energies).

In the following the choice of power-counting variables natural to our arbitrary pinch SP is made, and the corresponding homogeneous integral is discussed.

Choice of variables for cut vacuum polarization diagrams

A surface of pinch singularity points will be considered as being specified not only by the set of lines which go on-shell there, but also by its soft lines and the assignment of its finite-energy lines into jets. Figure 7 is a typical two-jet reduced diagram of a cut vacuum polarization graph.

Within the reduced diagram of a pinch SP, "jet" loops which pass only through finite-energy lines are distinguished from "soft" loops which pass through one or more zero-momentum line. As in Sec. II, the jet loops are chosen as a complete set

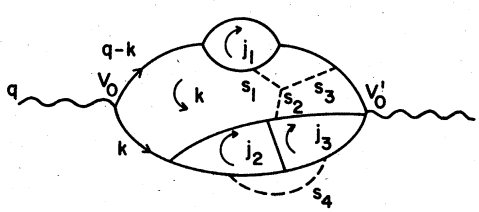

FIG. 7. Example of an SP illustrating the choice of normal variables.

of loops for the subgraph of the reduced diagram consisting of only the finite-momentum lines. In the particular choice of variables given below, jet and soft loops are considered separately.

Soft loops are treated in the same way as in the Euclidean case: All four components of each loop are chosen as normal variables. This is because pinch singularity surfaces with different numbers of soft lines are distinguished, and varying any subset of the soft-loop momenta will ensure that at least one soft line acquires momentum. In Fig. 7, for instance, three loop momenta must vanish in all four components to set the four soft momenta $s_1, \ldots, s_4$ equal to zero.

For jet loops it is easier to first identify intrinsic variables for an arbitrary pinch SP P on some surface of equivalent pinch SP's. These parametrize the variations δP for which $P+\delta P$ is on the same surface. Aside from leaving all lines on-shell, δP should not give momentum to any zero-momentum line, nor break up any jet. None of these things happen under translations which (A) vary the jet energies and directions or (B) redistribute energy among lines moving in the same jet.

Because each jet subdiagram begins at the same vertex (V_0 for the two jets in Fig. 7) and ends at the same vertex (V_0' in Fig. 7), jet loop momenta can be assigned so that, if there are n jets, $n-1$ loop momenta pass through more than one jet while the rest are internal loop momenta for individual jet subgraphs. In Fig. 7, where $n=2$, k is the only shared jet loop, while j_1, j_2 and j_3 are internal jet loops.

If all the lines of a jet subdiagram are to be on-shell, its external momentum must be lightlike. For n jets, this puts n conditions on the $n-1$ shared jet loop momenta. In Fig. 7 the two conditions are $(q-k)^2 = k^2 = 0$. These conditions being satisfied, the remaining $3n-4$ variables will determine the jet energies and/or directions (only the latter in Fig. 7), so by (A) they are intrinsic.

There are more intrinsic variables to specify, since translations of type (B) have not yet been considered. At this point it is useful to rotate into a different frame for each jet (while always staying in the external momentum c.m. frame). Let p_i denote the external momentum of the ith jet, and suppose that the shared jet loop intrinsic momenta have been fixed, and that $|p_i^2| \ll \max_\mu |p_i^\mu|^2$ (i.e., p_i is nearly on-shell). Then let F_i be the frame in which the transverse components $\vec{p}_i$ of p_i vanish, and where $p_i^- \gg |p_i^+|$. That is, in F_i, p_i is nearly lightlike and traveling in the $-z$ direction, and at the pinch SP all lines in the ith jet have nonzero minus components only. Corresponding to (B), then, the minus com-

ponent of each internal loop of jet i is chosen as an intrinsic variable, and similarly for all other jets. In Fig. 7 this means j_1^- in the frame where $(q-k)^+ = |\vec{q}-\vec{k}| = 0$, and j_2^- and j_3^- in the frame where $k^+ = |\vec{k}| = 0$. Of course, actually evaluating an integral with this choice of variables involves evaluating a complicated Jacobian. But the Jacobian will be nonsingular, since it comes from simple rotations, and will therefore not affect power counting.

The frames F_i are also used to define normal variables for the pinch SP P. To get all the lines of all the jets on-shell, it is necessary and sufficient to have all the external jet momenta light-like and parallel in spatial momentum to their respective external jet momenta (two conditions for each loop).

In F_i, then, normal coordinates are picked as p_i^+ for the external momentum of the ith jet, and $j_{k,i}^+$ and $|\vec{j}_{k,i}|^2$ for the kth internal loop of jet i. Left over are the azimuthal angles (in frames F_i) of each internal jet loop, which are undefined at the pinch SP, and which can be considered as intrinsic variables. Together with the other intrinsic and normal variables, this specifies a complete set of variables for the loop momenta of the reduced diagram.

Notice that the scale λ must be chosen the same for both soft and jet variables whenever a set L of jet lines carries soft momenta in addition to jet momenta. Since lines in L are linear in both jet variables and soft variables, choosing one set smaller than the other would result in many new surfaces of spurious SP's in the homogeneous integral.

V. POWER COUNTING FOR CUT VACUUM POLARIZATION DIAGRAMS

Having identified a set of normal variables, I will now go on to show that $p \geq 0$ for any pinch SP. This requires knowing the behavior of the homogeneous integral under scaling. For simplicity of presentation, I will postpone the discussion of vector particles and begin with nongauge theories. First, those pinch SP's are discussed whose reduced diagrams have only elementary vertices. Second, the inclusion of contracted vertex subdiagrams is discussed. Finally, I show how to extend the results to gauge theories. p is the sum of contributions from on-shell denominators, normal variable differentials, and numerator momenta.

Elementary vertices, no gauge particles

The homogeneous integral is constructed by neglecting terms quadratic in normal variables relative to linear terms. Denominators of soft lines will be quadratic, and denominators of jet lines will be linear, in the normal variables. Therefore, each soft denominator contributes a term -2 to p, and each jet denominator contributes -1.

Consider now an arbitrary pinch SP P with reduced diagram R_P. Let J and S be the number of finite- and zero-momentum lines in R_P, respectively, and suppose R_P has $L^{(s)}$ "soft" loops, $L^{(j)}$ internal "jet" loops, and K jets. Then

$$p = (4L^{(s)} + 2L^{(j)} + K) - (2S + J) + N, \tag{5.1}$$

where N is the contribution of numerator factors.

At this point it is useful to separate the effect of soft lines and loops in (5.1), which can be found by simple dimensional counting:

$$p = (2L^{(j)} + K - J + N^{(j)}) + b + \tfrac{3}{2}f, \tag{5.2}$$

where b and f are the number of soft boson and fermion lines attached to jet lines. Notice that if a single soft line is attached to hard lines at both ends (e.g., s_4 in Fig. 7) it is counted twice in b or f.

As will be seen below, $N^{(j)}$ can be written as $\sum_{i=1}^{K} n_i^{(j)}$, where $n_i^{(j)}$ is the numerator contribution from the ith jet. The quantity in parentheses in (5.2) can thus be expressed in terms of a sum over individual jets. In an obvious notation

$$p = \sum_{i=1}^{K} (2l_i^{(j)} + n_i^{(j)} - j_i + 1) + b + \tfrac{3}{2}f. \tag{5.3}$$

To put (5.3) into a more useful form, we use Euler's identity and the relation between the number of lines and vertices in each jet:

$$\begin{aligned} l_i &= j_i - v_i + 1, \\ j_i &= \frac{1}{2}\left(\sum_{\alpha \geq 3} \alpha x_{i,\alpha} + \sum_{\beta \geq 2} \beta y_{i,\beta} + \gamma_i + \delta_i\right). \end{aligned} \tag{5.4}$$

Here v_i is the total number of vertices in the ith jet, while $x_{i,\alpha}$ is the number of soft vertices in jet i with α jet lines and no soft lines attached. $y_{i,\beta}$ is the number of soft vertices with one or more soft lines, in addition to β jet lines, attached. Finally, γ_i and δ_i are the number of jet lines of jet i attached to the left- and right-hand hard vertices (V_0 and V_0' in Fig. 7). Using (5.4) and

$$\begin{aligned} v_i &= \sum_{\alpha} x_{i,\alpha} + \sum_{\beta} y_{i,\beta} + 2, \\ 2l_i^{(j)} + n_i^{(j)} - j_i + 1 &= \tfrac{1}{2}\sum_{\alpha \geq 3} (\alpha - 4) x_{i,\alpha} + \tfrac{1}{2}\sum_{\beta \geq 2} (\beta - 4) y_{i,\beta} \\ &\quad + \tfrac{1}{2}(\gamma_i + \delta_i - 2) + n_i^{(j)}. \end{aligned} \tag{5.5}$$

The next step is to find a lower bound for $n_i^{(j)}$.

We consider only theories without trilinear scalar couplings; the remaining three-point couplings must be fermion-scalar or pseudoscalar, with vertices proportional to the identity or γ_5. But each such vertex is sandwiched between a pair of fermion numerators. Let k be the momentum of the spin-zero line. Then there is a factor in the integrand of the form

$$(\not{p}+\not{k})(a_1+a_2\gamma_5)\not{p}=(a_1-a_2\gamma_5)(\not{p}+\not{k})\not{p}$$

which is associated with each three-point vertex. Suppose both fermion lines, of momenta p and $p+k$, are in the same jet. In the limit that p and $p+k$ go on-shell and parallel to the jet momentum, k is either vanishing or becoming proportional to p (if the boson line is also in the jet). In either case, the quantity $(\not{p}+\not{k})\not{p}$ vanishes at least as fast as the transverse components of the internal jet loop momenta on which p and $p+k$ depend. In terms of the variable λ, this gives a factor $\lambda^{1/2}$ in the numerator for each three-point vertex connecting three jet lines, or two fermion jet lines and a soft boson line. Let z_i be the number of vertices at which soft bosons attach to jet fermions. Then

$$n_i^{(j)} \geq \tfrac{1}{2}x_{i,3}+\tfrac{1}{2}z_i\,. \tag{5.6}$$

Substituting (5.5) and (5.6) into (5.3) gives

$$p \geq \sum_{i=1}^{K}\left(\tfrac{1}{2}\sum_{\alpha\geq 4}(\alpha-4)x_{i,\alpha}+\tfrac{1}{2}\sum_{\beta\geq 4}(\beta-4)y_{i,\beta}+\tfrac{1}{2}(\gamma_i+\delta_i-2)\right)$$
$$+\sum_{i=1}^{K}(-\tfrac{1}{2}y_{i,3}+\tfrac{1}{2}z_i-y_{i,2})+b+\tfrac{3}{2}f\,. \tag{5.7}$$

On the other hand,

$$\tfrac{1}{2}(b+f)\geq\tfrac{1}{2}\sum_{i=1}^{K}(y_{i,3}+y_{i,2})\,,$$
$$\tfrac{1}{2}f\geq\tfrac{1}{2}\sum_{i=1}^{K}(y_{i,2}-z_i)\,, \tag{5.8}$$

so that

$$p\geq\tfrac{1}{2}\sum_{i=1}^{K}\left[\sum_{\alpha\geq 4}(\alpha-4)x_{i;\alpha}+\sum_{\beta\geq 4}(\beta-4)y_{i,\beta}+\gamma_i+\delta_i-2\right]$$
$$+\tfrac{1}{2}(b+f)\geq 0\,, \tag{5.9}$$

as was asserted.

For $p>0$ the pinch SP in question gives no divergence at all, so (5.9) also supplies necessary conditions for divergence. These are

$$b=f=0\,, \tag{5.10a}$$

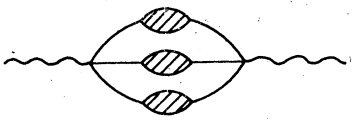

FIG. 8. Form of SP's which can give rise to mass divergences in theories without vector particles.

$$\gamma_i=\delta_i=1\,, \tag{5.10b}$$

$$x_{i,\alpha}=0\,,\quad \alpha>4\,. \tag{5.10c}$$

According to (5.10a), the reduced diagram of a divergence point can have no soft lines, by (5.10b) each jet must constitute a self-energy, and by (5.10c) no soft vertex may be of higher order than 4. [Notice that by definition (5.10a) implies all $y_{i,\beta}=0$.] Figure 8 illustrates the kind of reduced diagram associated with divergence in these theories. Notice that (5.10a) corresponds to the observation that Yukawa and ϕ^4 theories have no IR divergences in form factors.[13]

Contracted vertices

The next problem is to see what happens when one or more vertices of the reduced diagram of a pinch SP represent a set of contracted lines.

If all the external lines of the vertex are soft, then dimensional counting, after integration over the internal loops of the vertex, gives the same results as above.

Suppose the contracted vertex occurs in a jet subdiagram. First, (5.9) shows that if the order of the vertex is greater than, or equal to, four, it can lead to no enhancement of the integral. After integration over internal loops, two-point functions will be of the form $p^2f(p^2)$ or $\not{p}g(p^2)$ for spin-zero or $\frac{1}{2}$, with no worse than logarithmic divergences in f or g at $p^2=0$. (This is assuming that mass renormalization makes sense and has been carried out.) In both cases, the two-point function cancels a denominator and supplies a factor λ to the numerator to within logarithms.

Again after integration over internal loops, two-fermion-scalar vertices are of the form $f_1(t)+\gamma_5 f_2(t)$, where t denotes collectively the invariants formed from the external momenta. f_1 and f_2 are dimensionless, and can therefore diverge no worse than logarithmically. As for elementary vertices, a factor $\lambda^{1/2}$ is associated with ones for which both fermions are jet lines. From the above, it is easy to see that (5.9) is unchanged in the presence of contracted vertices.

Gauge theories

The extension of the above reasoning to gauge theories is complicated by the presence of un-

physical degrees of freedom. Consider, for instance, an elementary two-fermion-vector coupling of the form γ_μ. Then

$$(\not p + \not k)\gamma_\mu \not p = -\gamma_\mu(\not p + \not k)\not p + 2(p+k)_\mu \not p .$$

As seen above, the first term contributes a factor $\lambda^{1/2}$ to numerator scaling. The second, however, is unsuppressed. Suppose all three lines are in the same jet. In the limit that p and k are on-shell and parallel, p is proportional to k, and the vector line carrying k has an effective longitudinal polarization. It would be surprising if an unphysical degree of freedom could give rise to mass divergences, since divergences can be interpreted as resulting from degeneracies among physical states. If, in this case, longitudinal polarizations can be dropped, remaining terms will be of the order of transverse loop momenta, and will give a factor $\lambda^{1/2}$ to the numerator.

We know, of course, that all such unphysical degrees of freedom are in fact canceled after sums over gauge-invariant sets of graphs (in general including ghosts) are taken. They are, however, present on a graph-by-graph basis in covariant gauges, and individual graphs may be worse than logarithmically divergent. As a result, the approach developed above, describing divergences on a graph-by-graph and point-by-point basis, is not immediately applicable in covariant gauges. There exist, however, a set of noncovariant gauges in which divergences associated with unphysical degrees of freedom are eliminated within each graph individually.

Let us define such a set of gauges by means of gauge-fixing terms of the form $(1/2\alpha)(e^{i\theta}\partial_0 A_0 - \vec{\gamma}\cdot\vec{A})^2$, where $0<\theta<\pi/2$, and the limit $\alpha\to 0$ is taken. By the standard manipulations[14] this gives a vector propagator of the form

$$G^{(\theta)}_{\mu\nu}(k) = \frac{-i}{k^2+i\epsilon}\left(g_{\mu\nu} - \frac{k^{(\theta)}_\mu k_\nu + k^{(\theta)}_\nu k_\mu}{k^{(\theta)}\cdot k} + \frac{(k^{(\theta)})^2 k_\mu k_\nu}{(k^{(\theta)}\cdot k)^2}\right), \tag{5.11}$$

where for any vector a_μ, we define

$$a^{(\theta)}_0 = e^{i\theta}a_0, \quad a^{(\theta)}_i = a_i, \quad i=1,2,3. \tag{5.12}$$

The corresponding ghost Lagrangian is

$$\bar{\phi}\partial^{(\theta)}_\mu\partial^\mu\phi - g c^{abc}\bar{\phi}_a\partial^{(\theta)}_\mu A^\mu_b \phi_c , \tag{5.13}$$

so that the ghost propagator is

$$\Delta^{(\theta)}(k^2) = -i/k^{(\theta)}\cdot k . \tag{5.14}$$

The propagators (5.11) and (5.14) have a number of interesting properties. First, notice that

$$k^{(\theta)\mu}G^{(\theta)}_{\mu\nu}(k) = 0 . \tag{5.15}$$

$k^\mu G^{(\theta)}_{\mu\nu}(k)$ does not vanish, but has no pole in k^2, and in fact diverges only when $k_\mu = 0$, $\mu = 1,\ldots,4$:

$$ik^\mu G^{(\theta)}_{\mu\nu}(k) = -\frac{k^{(\theta)}_\nu}{k^{(\theta)}\cdot k} + \frac{(k^{(\theta)})^2 k_\nu}{(k^{(\theta)}\cdot k)^2} . \tag{5.16}$$

Equations (5.15) and (5.16) show that in these gauges there is no physical pole for either longitudinal or scalar polarization, and, in particular

$$i\delta_{\mu 0}G^{(\theta)}_{\mu\nu} = (e^{i\theta}-1)^{-1}\left(\frac{k^{(\theta)}_\nu}{k^{(\theta)}\cdot k} - \frac{(k^{(\theta)})^2 k_\nu}{(k^{(\theta)}\cdot k)^2}\right), \tag{5.17}$$

$$i\sum_{\mu=1}^{3} k^\mu G^{(\theta)}_{\mu\nu} = (e^{-i\theta}-1)^{-1}\left(\frac{k^{(\theta)}_\nu}{k^{(\theta)}\cdot k} - \frac{(k^{(\theta)})^2 k_\nu}{(k^{(\theta)}\cdot k)^2}\right).$$

Similarly, according to (5.11) and (5.14), the gauge terms and ghost propagator diverge only when their momenta vanish in all four components. Finally, notice that in the limit $\theta\to 0^+$ the ghost and vector propagators go smoothly to their forms in the Landau gauge. Taking θ finite is similar to taking ϵ finite in a subset of denominators of the form $q^2+i\epsilon$. The effect is always to move the corresponding energy poles away from the real axis without crossing the axis, so that integrals along the undeformed contour remain defined. It is also not difficult to verify that so long as $\theta<\pi/2$ the presence of $k^{(\theta)}\cdot k$ denominators does not interfere with Wick rotation for Euclidean Green's functions, although the resulting quantities are in general complex and noncovariant.

An important point is that the introduction of this gauge actually simplifies the catalog of pinch SP's found with a covariant gauge. This is because covariant denominators such as $k^2+i\epsilon$ in ghosts and gauge terms are replaced by $k^{(\theta)}\cdot k$, which vanishes only for $k=0$ on the undeformed contour. Therefore, no finite-energy on-shell ghosts appear at SP's, and gauge term denominators give no power-counting enhancement to integrals.

We can now count powers for pinch SP's with on-shell vector lines, using the fact that, by (5.16), longitudinal polarization does not propagate in the gauges we are using. As above, pinch SP's with only elementary vertices are considered first.

The relation (5.16) results in a suppression of order $\lambda^{1/2}$ for every elementary trilinear soft vertex where all three lines are in a jet. Such vertices may connect three vectors, or a vector and two fermion or scalar lines. In the first and third cases this follows immediately from the momentum-space forms of the vertices. In the second it follows from the fact that the vertex γ_μ leads to longitudinal polarization for the vector

line, as mentioned above. In contrast to the scalar-fermion case, however, there is no suppression associated with a vertex at which a finite-energy jet line emits a soft vector. The analog of (5.6) in a theory coupling vectors to charged fermions or scalars is thus

$$n_i^{(j)} \geq \tfrac{1}{2}x_{i,3} + \tfrac{1}{2}z_i^{(0)}, \tag{5.18}$$

where $z_i^{(0)}$ is the number of soft scalars emitted at three-point vertices by jet lines. Otherwise, the reasoning leading up to the bound (5.7) on p is unchanged, and for gauge theories we find

$$p \geq \sum_{i=1}^{K}\left(\tfrac{1}{2}\sum_{\alpha\geq 4}(\alpha-4)x_{i,\alpha} + \tfrac{1}{2}\sum_{\beta\geq 4}(\beta-4)y_{i,\beta} + \tfrac{1}{2}(\gamma_i+\delta_i-2)\right) + \sum_{i=1}^{K}(-\tfrac{1}{2}y_{i,3} + \tfrac{1}{2}z_i^{(0)} - y_{i,2}) + b^{(0)} + b^{(1)} + \tfrac{3}{2}f, \tag{5.19}$$

where $b^{(0)}$ and $b^{(1)}$ refer to soft scalar and vector lines, respectively, and where otherwise the notation is the same as above. Using the analog of (5.8),

$$p \geq \tfrac{1}{2}\sum_{i=1}^{K}\left(\sum_{\alpha\geq 4}(\alpha-4)x_{i,\alpha} + \sum_{\beta\geq 4}(\beta-4)y_{i,\beta} + \gamma_i + \delta_i - 2\right) + \tfrac{1}{2}\sum_{i=1}^{K}[b_i^{(0)} + (b_i^{(1)} - z_i^{(1)})] + \tfrac{1}{2}f, \tag{5.20}$$

where $z_i^{(1)}$ is the number of soft vector lines emitted by jet lines of jet i at three-point vertices. Since $b_i^{(1)} \geq z_i^{(1)}$, the right-hand side of (5.19) is positive. The conditions for $p=0$, and hence logarithmic divergence, are [compare (5.10)]

$$\begin{aligned} &b_i^{(1)} = z_i^{(1)}, \\ &b_i^{(0)} = f = 0, \\ &\gamma_i = \delta_i = 1, \\ &x_{i,\alpha} = y_{i,\alpha} = 0, \quad \alpha > 4. \end{aligned} \tag{5.21}$$

Equation (5.21) indicates the difference between theories with vector particles and those without. It shows that in the former case the reduced diagram of a divergence point may include soft lines, provided only soft vector lines attach to jet lines, and these only at three-point vertices. Notice, however, that soft fermion and scalar loops are not excluded, although they must not connect directly to finite-energy lines.

The extension of these arguments to include contracted self-energy and three-point vertices is somewhat more complicated than above because of the noncovariance of vertex graphs for $\theta \neq 0$. Consider, however, a single-loop contribution $V^{(G)}_{\mu\nu\lambda}$ to the three-vector interaction, corresponding to graph G. The Lorentz covariance of $V^{(G)}_{\mu\nu\lambda}$ has been broken only in the time component, and it still possesses rotational covariance. $V^{(G)}_{\mu\nu\lambda}$ may therefore be proportional only to vectors of the type $z_\alpha(\theta)$, where $z_\alpha(\theta)$ can be a complicated function of θ for $\alpha = 0$, but is a θ-independent linear combination of external spatial momenta for $\alpha = 1, 2, 3$. $V^{(G)}_{\mu\nu\lambda}$ may also be proportional to $g_{\alpha\beta}$, as well as $\delta_{\alpha 0}$.

Suppose that all the external lines of G approach the mass shell with finite momenta, according to the scale λ. Then (5.17) shows that each vector such as $z_\mu(\theta)$, or term such as $\delta_{\mu 0}$, appearing in $V^{(G)}_{\mu\nu\lambda}$ cancels a pole in one of the propagators connected to G. Hence, except for terms proportional to momenta transverse to the jet direction, every component of $V^{(G)}_{\mu\nu\lambda}$ cancels a vector propagator pole. We have already seen that pinch SP's involving the internal lines of G lead to no worse than logarithmic divergence, so the behavior of scalar functions of θ and the momenta need not be inquired into. The result is that any soft single-loop three-vector vertex connecting jet lines gives a suppression of order $\lambda^{1/2}$ to the integral, in the same way as an elementary three-vector vertex. Similar reasoning applies to a two-scalar-vector vertex, with the same result.

For a two-fermion-vector vertex Γ_μ at the one-loop level, we recall again that Γ_μ is taken between fermion numerators $\not{p}$ and $\not{p}+\not{k}$ where, at the pinch SP, $p^2 = p\cdot k = k^2 = 0$. If z is a vector of the type defined above,

$$\not{z}\not{p} = [z_0(\theta) - |\vec{z}|]\gamma_0\not{p} + O(\lambda^{1/2}), \tag{5.22}$$

where here $|\vec{z}|$ denotes the norm of all the space components of z. By rotational invariance, Γ_μ can have γ matrices in the form $\not{z}(\theta), \gamma_\mu$ or $\gamma_0\delta_0$. Also, because the fermions are massless,

$$\{\Gamma_\mu, \gamma_5\} = 0 \tag{5.23}$$

and Γ_μ must be odd in γ matrices. Therefore, the most general form is

$$\begin{aligned} (\not{p}+\not{k})\Gamma_\mu\not{p} = (\not{p}+\not{k})\big(&\gamma_\mu f_1(t^{(\theta)}) \\ &+ \delta_{\mu 0}\gamma_0 f_2(t^{(\theta)})\big)\not{p} \\ &+ O(\lambda^{1/2}), \end{aligned} \tag{5.24}$$

where $t^{(\theta)}$ denotes scalars formed from combinations of the z's. As with the three-vector case, we need not worry about singular behavior in the variables $t^{(\theta)}$, since such divergences must come from pinch SP's where the internal lines of Γ go on-shell, and these are already known to be no worse than logarithmic. Anticommuting $\not{p}+\not{k}$

past Γ_μ in (5.24), and using (5.17), we find here also a suppression of order $\lambda^{1/2}$.

Our conclusion is that (5.18), and therefore (5.20), continue to hold for pinch SP's with contracted single-loop three-point and higher jet vertices. The argument can now be iterated to include contracted vertices of arbitrary numbers of loops by treating at each step contracted vertices of lower order as "elementary" for power-counting purposes.

Self-energies for any line are of the form $\delta m(\theta) + G^{-1}(p)Z(p,\theta)$, where $\delta m(\theta)$ denotes a possible θ-dependent mass term, removed by renormalization, and $G(p)$ is the propagator. $G^{-1}(p)$ cancels one of the two external propagator poles. Notice that by (5.17), any term p_μ or $z_\mu(\theta)$ in a vector self-energy cancels a pole by itself. Every two-point function therefore supplies a suppression factor λ to the numerator near the pinch SP. Therefore, (5.20) is not changed by the inclusion of self-energies.

In summary, the power-counting estimate (5.20), and consequently the conditions (5.21) for logarithmic divergence remain valid for any pinch SP, with or without contracted vertices.

Feynman gauge

In the Feynman gauge, power-counting arguments are more indirect, since there is no analog of (5.16), and individual propagators can carry longitudinal polarization. Helicity conservation alone results in some suppression, corresponding algebraically to the fact that the scalar product of two momenta generated at vertices within the same jet vanish on-shell. It is not difficult to see, however, that there can still be power divergences on a point-by-point basis in the Feynman gauge. An example with two jets is shown in Fig. 9. All lines are vectors. At the SP in question, $s=0$, while $k_1^2=k_3^2=0$ and $l_1^2=l_1\cdot k_1=l_2^2=l_2\cdot k_3=0$. We are interested in the numerator factor where the momentum of each vertex u_i is carried by line k_i for $i=1,\ldots,4$ while the momenta of vertices u_5 and u_6 are contracted together by the propagator of the soft line. As a result, there is no numerator suppression at all, and the counting procedure outlined above indicates quadratic divergence at the SP. This example can be generalized to find (at worst) nth power divergence with n jets. In view of the above, however, power divergences do not appear in partially integrated cross sections. We can see this explicitly in the Feynman gauge by use of Ward identities.[15]

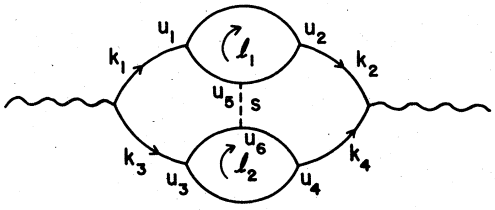

FIG. 9. Reduced diagram corresponding to an SP with quadratic divergence in the Feynman gauge. All lines are vectors; the dashed line carries zero momentum.

An SP at which power counting indicates nth-order power divergence must involve at least n longitudinally polarized vector lines, labeled $k_1,\ldots,k_n$. Each has propagator $g_{\mu\nu}/k_i^2$, but it is always possible to add a term $-k_{i,\mu}k_{i,\nu}/(k_i^2)^2$ to each line without affecting the cross section when $k_i,\ldots,k_n$ are held fixed but other momenta are integrated over, and a gauge-invariant set of graphs is summed over. This follows from the generalization of current conservation for non-Abelian gauge theories. In the Landau combination $g_{\mu\nu}-k_{i,\mu}k_{i,\nu}/k_i^2$, however, longitudinal degrees of freedom are absent. Although it gives zero overall, the second term eliminates longitudinal polarization in each case. Evidently, the contribution of longitudinal polarization in each line is zero as well, and all power divergences must cancel in the gauge invariant cross section.

Spurious pinch SP's

We can now return to the question of the effect of dropping nonleading terms in denominators when forming the homogeneous integral. The only terms of this type are soft transverse momenta (in frame F_i), which are dropped in the denominators of jet lines in the ith jet.

Neglecting these variables leads to a new set of pinch SP's in the homogeneous integral which are not present in the full integral. The simplest example is shown in Fig. 10. We are interested in the region near $k^2=k\cdot l=l^2=0$. In the homogeneous integral, $(l+s)^2$ is replaced by $l^2+2l^-s^+$. In the limit $k^2=k\cdot l=l^2=0$, the denominator $(k+l+s)^2$ will also vanish when $s^+=0$, irrespective of the other three components of s. The result is a pinch SP at the origin in the s^+ integral. The numerator momenta associated with vertices u_1

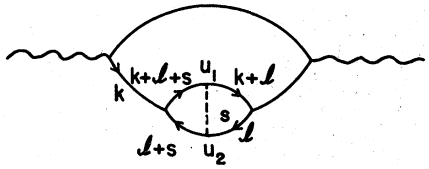

FIG. 10. Example for illustrating spurious SP. All lines are vectors; dashed line carries zero momentum.

and u_2 ensure that this pinch SP has associated with it only a logarithmic singularity. This homogeneous integral pinch SP, related to threshold singularities with massive particles,[16] is associated with an enhancement in the full integral when the pinch SP at $s=0$ is approached from the direction $s^+=0$.

This is easily generalized; the vanishing of n soft plus components s_i^+ can set as many as $2n$ jet lines on-shell, while numerator momenta and graph structure ensure at worst logarithmic divergence. This can be seen explicitly by starting out with a graph with on-shell jet lines, and then attaching soft lines arbitrarily.

VI. DISCUSSION

One thing to be emphasized from the foregoing discussion is the theory independence of the origin of mass divergences in cut vacuum polarization diagrams. Arguing from the nature of the momentum-space integrals which define Feynman diagrams, we were able to identify a common form for reduced diagrams of pinch SP's in any theory; the subset which actually gives rise to mass divergences depends on the numerator momentum and vertex structure of the theory in question. It is worth remarking on the role that gauge invariance plays in the case of gauge theories. It is necessary to eliminate contributions from nonphysical degrees of freedom, associated with power mass divergences, from cross sections. Taking this into account, we find at worst a logarithmic divergence in smeared cross sections.

This reasoning can be extended in several directions. First, it is not difficult to extend power counting to include massive lines. In this case, however, the rule of logarithmic divergences in smeared cross sections no longer applies when account is taken of threshold singularities.[16] Second, it is possible to apply the entire method to more complicated physical processes. Of particular interest are potential and four-particle scattering amplitudes. Here again contour integral considerations limit the structure of possible pinch SP's, and power-counting reasoning can be applied to limit divergence-causing regions still further.

ACKNOWLEDGMENTS

The author wishes to thank Shau-Jin Chang, Garland Grammer, John Stack, Roberto Suaya, and Jeremiah Sullivan for helpful conversations at various stages in the development of this work. This work was supported in part by the National Science Foundation under Grant No. PHY-76-15328.

APPENDIX: POWER COUNTING AT AN ARBITRARY SP

Although by definition integrals are not trapped except at pinch SP's in cut vacuum polarization graphs, it is always possible to ask what would happen if the contours were *constrained* to pass through a surface of SP's which were not necessarily pinch SP's. The singularity surface might be chosen to define the end points for finite integrals over loop momenta, for instance. In this appendix, it will be shown that power counting gives at worst logarithmic divergence for any SP whose reduced diagram contains no loop where plus momentum (or equivalently, energy) flows in the same direction as the loop momentum for every line in the loop. Such diagrams can be "ordered" so that plus momentum flows in the same direction for every line in the diagram. This result is important for a discussion of the cancellation of mass divergences.[6] The reasoning is applicable to more general scattering processes.

At an arbitrary SP the reduced diagram may be much more complicated than at a pinch SP because hard vertices can be present, and it need not represent a physically realizable process. Nevertheless, if the momenta of on-shell lines are real, the reduced diagram will fall into the same general form as for pinch SP's, consisting of jets of parallel-moving finite-energy particles along with a set of soft lines. In contrast to the case of a pinch SP, however, the jets may scatter in a nontrivial way, exchanging finite momenta, or changing direction altogether. Because of this, each jet may have a number of independent finite external momenta rather than just one. Each such independent external momentum may be carried by a single line, which, of course, is then on-shell.

To see how this possibility affects power counting at such an SP, consider a case where the ith jet has w_i external momenta ($w_i \geq 2$), each of which is carried by a single line. This is clearly the most singular case; the power counting at an SP where one or more external jet momentum is carried by more than one line is suppressed.

Power counting for soft lines is the same as at a pinch SP, and (5.3) is replaced by

$$p=\sum_{i=1}^{K}(2l_i^{(j)}+n_i^{(j)}-j_i)+A+b+\tfrac{3}{2}f\,, \tag{A1}$$

where A is the number of normal variables associated with external jet momenta. For a pinch SP, $A=K$, as in Sec. V. Going through the same reasoning as in Sec. V gives for a theory with gauge lines [compare (5.20)]

$$p \geq \tfrac{1}{2}\sum_{i=1}^{K}\Big[\sum_{\alpha\geq 4}(\alpha-4)x_{i,\alpha}+\sum_{\beta\geq 4}(\beta-4)y_{i,\beta} - 3w_i+4\Big] + A+\tfrac{1}{2}\sum_{i=1}^{K}[b_i^{(0)}+(b_i^{(1)}-z_i^{(1)})]+\tfrac{1}{2}f\,. \tag{A2}$$

If the right-hand side of (A2) is to be non-negative, we must have

$$A \geq \sum_{i=1}^{K}[\tfrac{3}{2}(w_i-2)+1]. \tag{A3}$$

Proving (A3) is basically a matter of counting.

Consider the reduced diagram R_P of an arbitrary SP P. R_P is made up of a soft lines as well as jets, but soft lines can be ignored for the purpose of this argument. In each jet i, contract every line in the jet to a point except $w_i - 1$ of the external jet lines, chosen arbitrarily. The resulting graph $\hat{R}_P$ is still a vacuum polarization graph, but it has only hard vertices. Using the fact that hard vertices to which no external lines attach are fourth order or higher, it is easy to show that

$$2L_{\hat{R}_P} - N_{\hat{R}_P} \geq 0\,, \tag{A4}$$

that is, that in $\hat{R}_P$ there are no more than two lines for every loop.

At the SP, all the external momenta $k_\alpha^{(i)}$ of jet i must be lightlike and parallel. As a result, all but one of them can be treated on the same footing as internal jet loops in Sec. IV. As in Sec. IV, a single external momentum $k_1^{(i)}$ defines a frame F_i in which $\vec{k}_1^{(i)}=0$. $(k_1^{(i)})^+$ is chosen as a normal variable. For $k_\alpha^{(i)}$, $\alpha>1$, $(k_\alpha^{(i)})^+$ and $|\vec{k}_\alpha^{(i)}|^2$ are normal variables. We will refer to $k_1^{(i)}$ as the "reference" momentum of jet i. Altogether, there are $2(w_i-1)-1$ normal variables, as expected. This does not necessarily mean that A equals $\sum[2(w_i-1)-1]$, because they need not all be independent. This is not a problem in Sec. IV, where the normal variables are simply components of internal jet loop momenta.

What we can do is to identify an independent subset of the normal variables; if there are

$$\sum_{i=1}^{K}[\tfrac{3}{2}(w_i-2)+1]$$

or more of them than (A3) is verified, and whatever the status of the remainder of the normal variables, divergences are at worst logarithmic.

With each loop γ of $\hat{R}_P$ associate a set S_γ of lines of $\hat{R}_P$. S_γ may consist of either one or two lines which carry the momentum of loop γ. The S_γ are chosen so that no line is counted twice and, if S_γ contains two lines, they are not both of the same jet. The idea is to choose the normal variables for the line(s) in S_γ from the four components of loop γ. This is clearly no problem if S_γ contains only one line. Suppose S_γ contains two lines $k_\alpha^{(i)}$ and $k_\beta^{(j)}$. A possible choice of variables is $(k_\alpha^{(i)})^+$, $|\vec{k}_\alpha^{(i)}|^2$, and $(k_\beta^{(j)})^+$. [Recall that $(k_\beta^{(j)})^+$ is defined in frame F_j while $(k_\alpha^{(i)})^+$ is defined in frame F_i.] If $(k_\alpha^{(i)})^+$ and $|\vec{k}_\alpha^{(i)}|^2$ are chosen from the components of γ, $(k_\beta^{(j)})^+$ will depend on other loop momenta as well as γ, in general. Nevertheless, for an ordered SP, it is not difficult to choose the loops so that the complete set of such variables is independent, as follows.

It is not hard to show that if R is ordered, $\hat{R}'$ can always be chosen so that there is at least one loop γ_1, attached to the initial vertex V_0, with only two lines (not both in the same jet). After choosing S_{γ_1} as above, we can contract γ_1 to form a new diagram $\hat{R}'$ with one less hard vertex than $\hat{R}$. The variables of $\hat{R}'$ may be chosen independently of those for γ_1, starting with just such another loop γ_2. This procedure can be continued until there is only one hard vertex left, and all the remaining S_γ can be chosen to have only one momentum each.

For any loop γ, if $k_\beta^{(j)}$ is the reference momentum of jet j this is a complete set of variables, but if neither $k_\alpha^{(i)}$ nor $k_\beta^{(j)}$ is a reference momentum this is one variable too few. Since $|\vec{k}_\alpha^{(i)}|^2$ involves two components of loop γ, it is not clear whether $|\vec{k}_\beta^{(j)}|^2$ is independent or not. The *minimum* number of independent variables that are chosen this way is

$$\sum_{i=1}^{K}[2(w_i-2)+1]-\tfrac{1}{2}\sum_{i=1}^{K}(w_i-2) = \sum_{i=1}^{K}[\tfrac{3}{2}(w_i-2)+1], \tag{A5}$$

when *every* nonreference momentum occurs in a set S_γ with another nonreference momentum (in this case, of course, $\sum_{i=1}^{K}w_i$ is an even number). This verifies (A3).

[1]C. N. Yang and R. L. Mills, Phys. Rev. 96, 191 (1954); H. Fritzsch, M. Gell-Mann, and H. Leutwyler, Phys. Lett. 47B, 365 (1973); D. J. Gross and F. Wilczek, Phys. Rev. D 8, 3633 (1973); S. Weinberg, Phys. Rev. Lett. 31, 494 (1973).

[2]C. G. Callan, Phys. Rev. D 2, 1541 (1970); K. Symanzik Commun. Math. Phys. 18, 227 (1970); S. Weinberg, Phys. Rev. D 8, 3497 (1973).

[3]T. Kinoshita, J. Math. Phys. 3, 650 (1962).

[4]T. D. Lee and M. Nauenberg, Phys. Rev. 133, B1549 (1964).

[5]D. Yennie, S. C. Frautschi, and H. Suura, Ann. Phys. (N.Y.) 13, 379 (1961); G. Grammer and D. Yennie, Phys. Rev. D 8, 4332 (1973).

[6]G. Sterman, following paper, Phys. Rev. D 17, 2789 (1978).

[7]T. Kinoshita, Ref. 3. See also T. Kinoshita and A. Ukawa, Phys. Rev. D 15, 1596 (1977); 16, 332 (1977). Other interesting approaches to the identification and evaluation of mass divergences can be found, for instance, in T. Appelquist and J. Carazzone, *ibid.* 11, 2856 (1975); J. M. Cornwall and G. Tiktopoulos, *ibid.* 13, 3370 (1976); 15, 2937 (1977); P. Carruthers and F. Zachariasen, Phys. Lett. 62B, 338 (1976); P. Carruthers, P. Fishbane, and F. Zachariasen, Phys. Rev. D 15, 3675 (1977); P. Olesen, Nucl. Phys. B104, 125 (1976); Phys. Lett. 66B, 370 (1977). E. Poggio and H. Quinn, Phys. Rev. D 14, 578 (1976); C. T. Sachrajda, *ibid.* 14, 1072 (1976); K.-J. Kim, Phys. Lett. 69B, 189 (1977); 69B, 347 (1977); N. K. Nielsen, Nucl. Phys. B124, 109 (1977); P. Cvitanović, *ibid.* B130, 114 (1977); T. Kimura and K. Kitago, Chiba Univ. report, 1977 (unpublished); J. Frenkel and R. G. Garcia, Phys. Lett. 73B, 171 (1978).

[8]For use of similar reasoning in a related context see G. Sterman, Phys. Rev. D 14, 2123 (1976).

[9]S. Coleman and R. E. Norton, Nuovo Cimento 38, 438 (1965).

[10]R. J. Eden, P. V. Landshoff, D. I. Olive, and J. C. Polkinghorne, *The Analytic S-Matrix* (Cambridge Univ. Press, Cambridge, England, 1966).

[11]J. M. Cornwall and G. T. Tiktopoulos, Ref. 7; J. Frenkel, R. Meuldermans, I. Mohammed, and J. C. Taylor, Phys. Lett. 64B, 211 (1976); C. P. Korthals-Altes and E. deRafael, *ibid.* 62B, 320 (1976); Nucl. Phys. B125, 275 (1977); P. Cvitanović, Phys. Lett. 65B, 272 (1976); J. Frenkel, *ibid.* 65B, 383 (1976); D. P. Crewther, Cal. Tech. Report No. CALT-68-556 (unpublished); K. J. Kim, Mainz Report No. 76/6, 1976 (unpublished); J. Frenkel, M.-L. Frenkel, and J. C. Taylor, Nucl. Phys. B124, 268 (1977); E. Tomboulis, Phys. Lett. 67B, 414 (1977); E. C. Poggio, Phys. Rev. D 16, 2586 (1977); 16, 2605 (1977); G. Sterman, *ibid.* 17, 616 (1978).

[12]G. Sterman, Ref. 11.

[13]T. Appelquist and J. Primack, Phys. Rev. D 1, 1144 (1970); G. Marques, *ibid.* 9, 386 (1974); L. L. Wang and M. Creutz, *ibid.* 10, 3749 (1974); S.-S. Shei, *ibid.* 11, 164 (1975); G. Tiktopoulos, *ibid.* 11, 2252 (1975).

[14]G 't Hooft and M. Veltman, CERN Report No. 73-9 (unpublished).

[15]G 't Hooft, Nucl. Phys. B33, 173 (1971).

[16]T. Appelquist, M. Dine, and I. Muzinich, Phys. Lett. 69B, 231 (1977); Phys. Rev. D 17, 2074 (1978).